UNIVERSITY OF ILLINOIS

May 15 19 89

THIS IS TO CERTIFY THAT THE THESIS PRI PARED UNDER MY SUPERVISION BY

Loretta Y. Chou

ENTITLED Characterization of Shear Moduli and Viscosity

for Hard Sphere Silica Suspensions

IS APPROVED BY ME AS FULFILLING THIS PART OF THE REQUIREMENTS FOR THE

DEGREE OF Bachelor of Science in Chemical Engineering

Instructor in Charge

APPROVED: Richard Ackine

HEAD OF DEPARTMENT OF Chemical Engineering

O-1364

CHARACTERIZATION OF SHEAR MODULI AND VISCOSITY FOR HARD SPHERE SILICA SUSPENSIONS

by

LORETTA Y. CHOU

THESIS

for the

Degree of Bachelor of Science

in

Chemical Engineering

College of Liberal Arts and Sciences
University of Illinois
Urbana, Illinois

1989

Acknowledgements

I would like to express my thanks and appreciation to my advisor, Dr. Charles F. Zukoski for his support and inspiring enthusiasm throughout the course of this thesis.

I would also like to especially thank Louise Marshall for all her time, patience, and help.

Lastly, I would like to thank Liang Bin Chen, Dan Klingenberg, and Greg Bogush for all their patience and help in clarifying my many questions.

Table of Contents:

Table of Contents (continued)

List of Tables:

List of Figures:

General Introduction

The study of interparticle forces in hard sphere systems is important to the development of high quality ceramics. Since various factors including particle size, volume fractions, and temperature can alter the particle-particle interaction and in turn, effect its rheological properties, a clearer understanding of the relationship between these factors and the corresponding viscoelastic behavior can eventually lead to better processing methods.

The goal of current research in this area is to develop a correlation between shear moduli and particle size of a given volume fraction. From this, values of elasticity can be accurately predicted which would improve already existing ceramic processing techniques.

Specifically, the project can be divided into three parts. The aim of the first part of the project is to relate volume fractions of hard sphere silica particles to a measurement of elasticity, the shear modulus. Effects of particle size distribution are also studied. The second portion of the research is devoted to studying the attractive interaction forces between hard core silica particles resulting from temperature variations. Shear moduli values are measured as a function of temperature for various volume fractions and particle sizes. Concentrated suspensions of sterically stabilized silica are studied in order to characterize shear-dependent viscosities as a function of temperature for the final part of the research project; in addition, effects of particle size and volume fractions are investigated. For all experiments, silica suspensions which are rendered organophilic with grafted octadecyl chains and dispersed in decalin are used.

PART 1: Particle Size and Volume Fraction Dependency of Shear Moduli for Hard Sphere Silica Systems in Decalin

1.1 Background and Theory-

The shear modulus, G, or elasticity, of a concentrated suspension can be thought of as a way to characterize the bonding strength between particles. One can imagine a spring connecting two particles---it is the corresponding spring constant, k, which is related to the shear modulus. If a stress is applied momentarily, the two particles are "stretched" apart and away from one another; then once the stress is turned off, the spring relaxes and the particles return to their original equilibrium positions. The relaxation time, in effect, indicates the elasticity of the sample.

Shear moduli values are measured using a Rank Pulse Shearometer. The sample is placed in the cell between two parallel plates and a 200 Hz frequency sinusoidal signal initiates a shear wave at the upper crystal. After being propagated through the sample, the resulting wave is received by the bottom crystal which measures the change in the arriving wave. A diagram of the apparatus is seen in Figure 1. In theory, the storage component of the shear modulus can be calculated from the following formula:

$$G' = [V^2 p(1-n^2)] / (1+n^2)$$

where V is the propagation velocity of the shear wave in m/s, p is the density of the material in kg/m^3, and n is the ratio of the wavelength to the critical damping length. However, the shearometer works in a region where n is small. Thus, the equation can be simplified to:

$$G = pV^2$$

where G is the limiting value reached at high frequency [1].

The Rank Shearometer measures the time in which the travelling wave propagates between the sending and receiving plates which are set at a given distance apart; thus, the more elastic the suspension, the faster the wave is propagated throughout the sample since the particles are relaxed very quickly back to their equilibrium position.

The shear modulus can be split into two parts: the storage modulus ,G', and the

loss modulus, G". Both can be related by the following equation:

$$G = G' + iG''$$

where i is a constant equal to $(-1)^{1/2}$. The storage modulus, G', represents the energy which is elastically stored in the colloidal system, whereas the loss modulus, G", is a measure of energy lossed due to heat dissipation [2].

In the high frequency limit, G can be approximated by G', the storage modulus, as seen above. For this approximation to hold, the shear moduli values taken must be within an adequate high frequency region, G^{∞}, where all of the shear modulus potential energy can be incorporated into the storage component and relatively little is lost. In this way, all data obtained for various sizes can be compared on the same basis.

1.2 Review of Literature-

Related work by Buscall et al [3] and Chang [4] have demonstrated the effect of charged particles on high frequency shear moduli over a range of volume fractions and particle sizes.

In polystyrene lattices, Buscall has determined that the rheological behavior in these types of charged systems are viscoelastic. With the use of shear-wave propagation to measure elasticity, they found that as interaction between particles were increased through concentration, shear moduli values increased almost exponentially. In addition, certain variables including electrolyte concentration and particle size affected the values of shear moduli. An increase in concentration of electrolytes such as sodium chloride was found to lower the shear moduli by effectively shielding the charge, thus reducing the repulsive forces between the particles. The increase in particle diameter for a constant volume fraction also resulted in a lower elasticity since the center-to-center distance of separation is greater.

Although the effect of particle size was investigated, Buscall studied particle diameters within the range of 50-200 nm only. Furthermore, volume fractions used in their experiments were at a maximum of only 0.40. It was predicted, however, that at larger diameters above 200 nm, lattices would approach a close-packed limit before moduli could be measured.

Chang studied monodisperse suspensions of charged silica particles at a much higher range of particle sizes. The curves obtained for shear moduli as a function of volume fraction followed closely that of Buscall's, although a higher volume fraction was observed as a result of larger particle diameters. For a range of 241 to 551 nm particle diameters, volume fraction regions increased from over 0.40 to approximately 0.55. Electrolyte concentration effects were also observed for small diameter particles; shear moduli values were higher at lower ionic strengths as a result of a larger double layer which increases the extent of interaction. However, data points for large particle diamters fell within the same region, independent of the electrolyte ionic strength. These particles appear as hard shperes without charge; the effects of screening of the negative charge with large diameter particles are not observed as for the smaller particles.

In addition to homogeneous suspensions, mixtures were also investigated. It was originally expected that data for mixtures would fall within the outer limits set by the homogeneous data making up the mixture. However, in all cases but one, the shear modulus was lower for constant volume fraction than for either single large or small particles. No direct correlation was observed, yet it was thought that since large-large particle interactions dominated, the addition of small particles only decreased the shear modulus by increasing the total volume fraction.

1.3 Experimental-

1.3.1 Synthesis and preparation of non-aqueous silica particles

The method for the synthesis of monodisperse, colloidal silica used here was developed by Stober, Fink, and Bohn [5]. Particle sizes of approximately 100 and 200 nm were synthesized.

A 4.0-liter Pyrex reaction kettle is placed in a constant water bath at 55 deg. C. Reactants include tetraethyl orthosilica (TEOS), ammonia, ethanol, and water and are added in specified amounts pertaining to a "recipe" for predictable particle sizes and continually stirred. Bogush et al [6] determined specific correlations which can be

utilized to predict these final particle sizes within a narrow distribution; a maximum size of 800 nm can be achieved.

In addition, Bogush describes a seeded growth technique in order to increase solid content and growth of the particles in the dispersion. The technique involves an initial "seed suspension" and periodic additions of TEOS and water in a 1:2 mole ratio until the desired particle size is reached. Distilled TEOS is required only in the initial formation of silica particles.

The technique for rendering the silica particles organophilic was referenced from Van Helden et al [7] and slightly modified in the purification process. Prior to adding the stearyl alcohol for esterification, approximately 1-2 liters of ethanol was added to the silica particles in a 5.0 liter Erlenmeyer flask and boiled until the reflux vapors reached a temperature of 80 deg. C. The purpose of this step is to ensure the absence of any water and that the concentration is at the azeotrope. Octadecyl, or stearyl, alcohol is added and refluxed until the mixture reaches a temperature of 200 deg. C or more; thus, most of the ethanol is now boiled away. The esterification process occurs during a continuous reflux for approximately 4 hours.

Once esterification is complete, the particles were redispersed in chloroform with heating, and then centrifuged at 5,000 rpm. Originally, it was thought that a centrifuge time of one hour was sufficient for sedimentation of all particles. However, it was discovered later that the time was actually inadequate since many particles were still observed to be present in the supernatant.

Lastly, the supernatant was drawn off by vacuum distillation and chloroform was again added to redisperse the particles in order to purify the sample. The process described above was then repeated approximately 4 to 5 times until no trace of stearyl alcohol was left in the particles.

1.3.2 Shear Modulus Measurements

In preparation of the shear modulus work, the cyclohexane in which the sample of 350 nm particles was suspended in, was evaporated using a rotovap and then the particles were redispersed in a higher boiling solvent, decalin. It was observed that with a very small amount of decalin added, a relatively large change in the structural

properties resulted in a freer flow of the sample. The sample was once again concentrated with the rotovap to a volume fraction of approximately 0.58.

Shear moduli values were taken with a Rank Pulse Shearometer. Initially, the plates were zeroed at a point where they were just barely touching. The sample was then placed in the cell and the gain and sensitivity dials were varied in order that a maximum signal was received at the farthest plate distance. Care was taken to avoid changing the original settings of the dials during measurements so that calculations of G' and G" may be determined later. A value of 1,000 was inputed initially for the density and later corrected for by using the real value of 1.776 g/cm^3. Once the plate distance was set to the desired value, a measurement was taken. The plates were then brought closer by rotating the top screw by 0.5 mm and an equilibrium time of 1 1/2 hours was allowed before continuing another measurement. A minimum of ten consecutive points were taken at intervals of 0.5 mm plate distances. Thus, the shearometer calculated a slope of the linear plot produced and estimated a value of shear moduli. (Figure 2)

Once the corresponding shear modulus was determined, a small sample was taken with a spatula from the cell and placed in a pre-weighed vial and tightly capped. The vial with the sample was then weighed and left in the oven to dry at 80 deg. C. for approximately 4 days in order to determine the mass fraction. From the value of mass fraction, a corresponding value of volume fraction was calculated using particle and solvent density. Through this method, a curve of shear moduli versus volume fraction for the 350 nm particle sample was determined, as seen in Figure 3. Relevant data can be found in Table 1.

1.4 Results and Discussion-

1.4.1 Shear Modulus Measurements

Several problems were encountered during the shear moduli measurements. Due to the high concentrations in our experiment, samples were very rigid with virtually little flow observed. It was difficult to determine in this high volume fraction region whether the sample being measured was truly homogeneous throughout. From Figure 3, a wider scattering of data points is observed near the high volume

fraction end than in the lower volume fraction end. Since the more dilute sample does not support the propagation of shear waves as well, more erroneous data would be expected in this region. However, the scattering at the high end instead may be explained by the difficulty in maintaining a continuous homogeneity throughout the sample.

Another difficulty encountered was also attributed to the highly concentrated sample. Although proper care was taken to obtain samples for mass fraction determinations as quickly as possible, a certain amount of water was probably absorbed from the air into the sample; this would result in additional weight which would throw off the measured mass fraction and volume fraction determinations. In addition, the original drying time for mass fraction calculations was set at 48 hours. However, data indicated that a small, but significant change in mass was still observed. By trial and error, a drying time of approximately 4 days was used to maintain a constant mass.

Referring to Figure 3, the shape of the curve is similar to those found from the work of Chang [4]. Yet, for an approximate constant particle size, a higher volume fraction was observed for the hard sphere systems than the charged particles. For the charged particles of 368 nm in diameter, a narrow range of 0.47 to 0.53 was observed for the volume fraction. On the other hand, for a slightly smaller hard sphere particle diameter of 350 nm, a higher range of 0.52 to 0.58 was observed. This result can be explained by the interparticle repulsive forces seen in the charged suspensions. In charged silica particles, a like-charge repulsion occurs, which would maintain a greater distance between two particles, or effectively a raised volume fraction. In hard sphere systems, the particles can be packed much closer before interacting; thus, a higher volume fraction can be observed as a result.

Lastly, we were interested in trying to reach an even more concentrated sample, above the 58% volume fraction already reached, in order to observe the expected rise in shear modulus. Although the shear moduli values were much higher as expected--- approximately 900 Pa (uncorrected)--- volume fraction determinations were still under 58%. It could only be assumed that the error in the mass fraction determinations was due to the very high concentration as aforementioned.

1.4.2 Storage and Loss Components of the Shear Modulus

From calculations of both G' storage and G" loss using the previous data taken, it was found that our shearometer at a frequency of 200 Hz was not high enough to reach G_∞, as seen in the plot versus volume fraction, Figure 4. Table 2 lists the experimental numbers calculated.

A significant portion of the shear modulus is found in the loss component; thus, G cannot be approximated by G' with the use of our shearometer. It was calculated that for even smaller diameter particles such as 76 nm, a much higher frequency of 2,025 Hz is required to reach G_∞.

1.5 Conclusion-

From the result of our experimentation in shear modulus components, we found that at a frequency of 200 Hz, a consistent basis at G_∞could not be reached due to the high values of G" loss. Thus, we were forced to redirect our aim to characterize the relationship between shear moduli, volume fraction, and particle size. Instead of the hard sphere repulsions observed in our previous work, we now turn to the study of attractions between the particles resulting from temperature dependence.

PART 2: Temperature Dependency of Shear Moduli for Hard Sphere Silica in Decalin

2.1 Background and Theory-

Jansen, De Kruif, and Vrij [8] investigated the attractive term of the interaction potential of hard sphere silica systems. Without a temperature change, the repulsive term dominates; this is due to the stabilizing layers of octadecyl chains which are densely packed and as a result, cannot interpenetrate. However, Jansen et al have varied the interaction potential of hard sphere silica systems from repulsive to moderately attractive by changing the temperature of the system.

It has been found that the interactions between the stabilizing chains and the solvent are temperature dependent. By altering the properties of the solvent through a temperature change, the stability of the solvent-chain system can be varied. In steric stablization, the interaction between solvent and chain segments are attractive; the chain segments prefer contacts with the solvent molecules rather than other chains. However, if the chemical nature of the solvent is altered so that now chain segments and solvent molecules are repulsive, chain segments would prefer other chains and begin to aggregate together. Hence, a phase separation would occur. In our systems with decalin, Jansen has determined that at an instability temperature of 4 deg C., the phase separation actually appears as a gel in which the sample does not flow. In addition, the relatively short chains of our systems would result in a narrow temperature range where attraction would dominate.

Another way of viewing the physical state of action between particles from decreasing the temperature is in relation to the Van der Waals interaction potential and energy-distance curves. By decreasing the temperature, the potential well is essentially made deeper; thus, particles are in effect trapped and cannot move apart from their solid-like lattice unless sufficient thermal energy was present. Moreover, particles tend to flocculate easier if the particle diameters are large in comparison to the length of the hairs. This in effect produces a deeper potential well also,and in turn, larger particles will even flocculate independently of temperature.

2.2 Review of Literature-

Chen and Russel [9] studied the flocculation of hard sphere colloidal suspensions as a function of decreasing temperature. In their experiment with 50 nm particles in hexadecane, they have determined the relationship between the gelation, or phase transition, temperature and the volume fraction to be proportional--- an increase in the volume fraction results in an increase in the gelation temperature. The structure of the suspension is dependent on both the volume fraction and the temperature; the low frequency plateau modulus was found to increase as the sample of the temperature was decreased.

2.3 Experimental-

Shear moduli measurements were taken by using the Rank Shearometer in the same manner as described in Part 1. However, an additional component, a temperature glass jacket was incorporated as a part of the cell in order to control and maintain a constant sample temperature. (Figure 1)

The temperature was controlled by a heating unit-oil bath which circulates glycol at the desired temperature range of approximately 5 to -15 deg. C. The sample was allowed to reach a constant temperature for about 1 1/2 hours after changing the plate distance to ensure equilibration throughout the sample before taking measurements. In addition, the sample was allowed to warm up to room temperature and then cooled back down to the desired temperature for each set of measurements. A cooling time of approximately 5 hours was used.

Shear moduli was measured as a function of temperature for a range of volume fractions and different particle sizes.

2.4 Results and Discussion-

Various problems were encountered during measurements of shear moduli as a function of temperature. The time allotted in order to ensure temperature equilibrium and homogeneity throughout the sample in between temperature changes was found to be insufficient. From cooling the sample overnight, more consistent readings were produced, thus indicating that a longer time period was needed to assure that the

phase transition had occurred through to the center of the shearometer plates. In order to determine the cooling time required, the Gurney-Lurie chart was used for a long cylinder. [10] An approximate cooling time of 5 hours was calculated based on the similar properties of benzene.

Another problem observed was the relatively large temperature fluctuations on the order of approximately ± 2-3 degrees C. seen in the refrigerated bath. Measures were taken to correct the problem; insulation composed of glass wool and aluminum foil was used to cover the inlet and outlet tubing which connected to the temperature jacket and bath. Although a fluctuation in temperature was still present, it was reduced to an order of only ±1 deg. C.

Another difficulty found during measurements was suggested by the irregularity of the curves obtained by the shearometer. This irregularity could be due to insufficient time for re-equilibration of the sample after altering the plate distance in between readings. The very cold temperatures we were working with usually resulted in a very "solid" sample which did not flow easily; the rigid sample may have been disrupted to a point where it cannot re-equilibrate again.

Lastly, difficulties in maintaining a constant volume fraction between temperature changes were encountered. For two successive runs, a significant difference of 0.464 to 0.484 volume fraction was observed. Data taken was observed to be highly sensitive to a slight change of volume fraction. Measures taken to reduce evaporation of the decalin solven included covering the inside of the bottle cap with Teflon tape and periodic cleaning of the jar.

More dilute suspensions were utilized in these sets of experiments than those in part 1. Dilute suspensions in the first part prevented the Shearometer from detecting any signal at all; however, by using relatively dilute systems here, attractive interactions due to temperature variations can be studied. Since the physical state of the suspensions are very sensitive to volume fraction changes, volume fractions slightly under 50% were sufficient to be considered dilute. In other words, the suspensions were "runny" at approximately 48% and could be used in the temperature variation experiments whereas slightly higher volume fractions of only 52% were almost solid-like in character and were used in experiments from part 1.

Initial data taken with 350 nm silica particles are shown in Figure 5. The curve corresponds to original expectations-- the curve follows an exponential-like form and extremely high values of shear moduli are observed at very low temperatures. For example, shear moduli values of approximately 51,000 Pa (uncorrected) are noted at a temperature of -10 deg. C, whereas the maximum shear modulus observed in the previous experiments of part 1 were seen at only 873 Pa (corrected). On the contrary, however, the curve shown in Figure 5 proved to be inaccurate since large temperature fluctuations in the bath were not accounted for in the measurements. After insulation of the equipment, measurements were again continued.

Subsequent data taken for 350 nm silica particles is summarized in Table 3. As can be seen, a large amount of data points are very inconsistent or obscured by noise. This could be due to insufficient cooling and also to the dilute nature of the sample. In a comparison of recent data to that of the previous data in Figure 5, the shear moduli versus temperature curve now seems to display a very steep drop within a narrow temperature range and then immediately flattens out; this result is contrary to the original exponential-like curve obtained before. In addition, the volume fraction is not constant throughout the measurements which could have also caused inconsistencies in the data.

Due to a significant loss and contamination of the 350 nm particles, measurements were taken on a suspension of 700 nm particles. Moreover, the effect of increasing particle sizes on shear moduli could be observed. For a volume fraction of 0.505, the shear modulus was determined to be very high--22,176 Pa-- at a temperature of -13 deg C. However, at a small temperature change to -10 deg. C, measurements could not be taken and signals were nearly imperceptible.

2.5 Conclusion-

Although much of the data obtained were inconsistent to expected results and theory, a summary of the results still indicate a very steep drop in the shear modulus occurs within a narrow temperature range. However, due to strong inconsistencies, our aim was redirected towards studying temperature effects on another viscoelastic property, the viscosity.

PART 3: Variations in Temperature for Shear-Dependent Viscosities of Hard Sphere Silica Systems in Decalin

3.1 Background and Theory-

Viscosity can be thought of in simplistic terms as a property which describes the ability to shear planes of particles against one another. A highly viscous suspension would require a higher stress to make the particles move in relation to each other versus a lower viscosity suspension. If a constant shear stress is applied in one direction at the top layer of particles in a suspension, a velocity profile throughout the suspension would be observed. This velocity profile decreases much more rapidly between particles in a viscous medium than in a less viscous one; in other words, a rapidly decreasing velocity profile between particles essentially retards movement of adjacent particles.

Figure 6 shows a typical curve of a viscosity-shear stress plot for hard sphere systems. At low stresses, a plateau is observed; the suspension acts as a Newtonian liquid in which flow can still be observed . Particles are randomly spread so that they collide into one another due to Brownian motion as stress is applied. Since the shear stress is low, however, the collisions are not very strong and shearing is not prevented. In the decreasing portion of the curve, particles begin to order into layers which facilitates the flow as the shear stress increases; thus, the viscosity decreases---this phenomenon is called shear thinning. Finally, at the high stress plateau, a highly ordered state of particles can be observed in which layers of particles slide past one another with a low resistance.

In contrast to shear thinning, suspensions may also show the process of shear thickening. Physically, at high shear rates, particle vibrations begin to overcome the ordered layering and the particles become disordered once again; thus, the viscosity begins to increase at higher stresses. Shear thickening is more readily observed for larger diameter particles and higher volume fractions. As particle size and volume fraction decrease, shear thickening can still be observed but at much higher shear stresses.

In Figure 7, the exponential increase in viscosity at very low shear stresses shows

a solid-like character. The stress at which viscosity is infinite is known as the yield stress. By decreasing the temperature so that the attractive interaction potential predominates and in turn, the particles weakly flocculate, the suspension is expected to eventually reach a solid-like state as shown in Figure 7.

3.2 Review of Literature-

Related work in the area of volume fraction effects on shear-dependent viscosities are studied by Papir and Krieger [11], Woods and Krieger [12], and Marshall and Zukoski [13].

Woods et al investigated aqueous dispersions in steady shear flow. Non-Newtonian viscosities of monodisperse polystyrene and polyvinyltoluene latexes were measured as a function of electrolyte level and shear stress at volume fractions up to 0.50. Effects of stress, concentration and particle sizes were studied also. Typical curves of viscosity versus shear stress at various electrolyte contents and corresponding crossplots reveal that there are strong electrolyte effects at low shear stresses, a distinct minimum at a shear stress-independent electrolyte level, and a high shear limiting viscosity which is independent of electrolyte content.

Perhaps most interesting is their study on effects of particle diameters on Non-Newtonian viscosities of uniform sphere dispersions. Various particle diameters ranging from 0.2 to 0.8μ were prepared at an effective concentration of 0.50; surfaces were saturated with 95% surfactant and suspensions were neutralized in terms of pH. It was discovered that curves of stress -dependent viscosities fell in three distinct curves for particles smaller than 0.5μ, whereas data for the two larger particle diameters were superimposed onto one another. For the larger particles, it was concluded that hydrodynamic forces and the forces of Brownian movement play an important role. According to their data, only particle sizes below 0.5μ in diameter can be considered in aqueous dispersions to behave as independent rigid spheres.

Investigations by Woods et al were extended to dispersions in non-aqueous media. Papir et al obtained rheological data for four different particle sizes ranging from 0.155μ to 0.433μ in diameter in organic media of benzyl alcohol and m-cresol.

Upon changing the shear stress to the dimensionless reduced shear stress,

$$\tau_r = \tau a^3 / (kT)$$

data points for both media superimpose onto a single curve at a given volume fraction. Thus, Van der Waals and coulombic forces are observed to be overridden by Brownian movement and shear stress effects.

In a comparison of results between Papir and Woods, coulombic forces which act on particle interactions are much weaker for the non-aqueous media; this is observed since it is not necessary to shield charges in order to achieve superposition of the curves.

Marshall and Zukoski studied suspensions of hydrophobic silica particles near close packing. They have found that viscosities are independent of shear stress at low volume fractions for particle diameters of 210 nm ± 10, yet at volume fractions above 0.5, the samples show shear thickening, or an increase in viscosity at higher stresses. Zero shear rate viscosities were determined for various volume fractions and were found to greatly increase within a narrow range of 0.55-0.60. However, even at such a rapid increase in the zero shear rate viscosities, plateaus were observed for every volume fraction; this indicates that the samples behave as Newtonian liquids in which flow can still be observed.

3.3 Experimental-

Shear-dependent viscosity data are taken by a Bohlin Constant Stress Rheometer, incorporating a C25 size cup and bob system in order to measure higher shear stresses. A diagram of the principle components is shown in Figure 8. In order to minimize the possiblity of solvent evaporation which would change the volume fraction of the sample, a solvent trap device is added to the rheometer. Decalin is periodically added to the bottom portion of the trap to maintain the solvent at a consistent level. In addition, a thermostat unit is attached to control and maintain a constant temperature throughout the sample. However, since this thermostat unit reaches a minimum temperature of only 5 deg. C , a recycling refrigerated bath utilizing glycol is intermittently substituted for working at much colder temperatures.

The rheological property, viscosity, is measured using a different approach than the one for elasticity. Once the cup is filled with the suspension, the bob is lowered until the sample covers its entire surface. A constant stress, set through the computer, is then applied to the suspension in the cup by a bob which rotates on a low friction air bearing. The variation in shear stress is computer controlled; consecutive stresses are swept from low values to high values with a constant time interval between each measurement to ensure equilibrium within the sample. An integration time period is chosen in order that the shear rate has adequate time to approach steady state.

Various temperature-dependent viscosity versus shear stress curves were determined at three consequently more dilute samples for 700 nm particles; in addition, a run was made for a 112 nm particle diameter suspension.

3.4 Results and Discussion-

Viscosity versus shear stress curves can be seen in Figure 9 for five different temperatures. Since the particle size was relatively large--700 nm-- low stress measurements were not made due to inadequate time for the system to reach steady state. Thus, the figure displays only a moderate range of stresses. Low and high end values on the curve, however, reveal deviations from the average for cold temperatures at 0.7 deg C. At the low stress end, the curve begins to climb exponentially-- this result corresponds to the expected outcome in which very cold temperature suspensions would show an infinite viscosity and a yield stress. Another observation can be made at the high stress end; increasing viscosity indicates a slight shear thickening of the suspension for the cold temperature curve. An explanation centers upon the fact that by increasing the volume fracti . or by decreasing the temperature, both processes would in effect result in ,ser particle-particle interactions. Since an increase in volume fraction increases the probability for shear thickening, a colder temperature would essentially do the same. Hence, the presence of shear thickening at colder temperatures is understood.

The curve in Figure 9 also shows expected trends; a higher temperature results in a lower viscosity at a given shear stress. Thus, the curves are shifted accordingly for various temperatures. In addition, comparisons between Figures 9 through 12 for

different volume fractions reveal outcomes which can be predicted by theory. For instance, lower volume fractions at constant stress and temperature yields lower viscosities.

Near the high stress region in Figure 9, curves corresponding to temperatures of 9.3, 13.4, and 25 deg. C are superimposed upon one another. Bonds between particles are broken at higher shear stresses, thus reducing the viscosity to being stress independent. However, a difference in viscosity for the colder temperature curves is seen in a comparison to those curves which are superimposed. This difference observed may be a result of viscosity changes due to temperature variation for the solvent, rather than for the particles themselves. The change in viscosity seen is approximately on the order of 1 PaS.

In the second set of experiments corresponding to Figure 10, the sample was diluted in order to change the volume fraction of the suspension. However, volume fraction measurements indicated a higher volume fraction of 0.512 instead of a lower one. One possiblity of this inconsistency can be due to the sample being weakly flocculated within the cup; therefore, a sample taken for volume fraction measurements may not be indicative of the true value. Large particle sizes of 700 nm tend to flocculate independent of temperature. An independent observation of the 700 nm particles showed an appreciable amount of flocculation upon storage for more than a day.

In Figure 12, measurements were taken for smaller particle diameters at 112 nm. A full stress sweep was made for each temperature in order to study low and high stress effects. Note that each curve shows a slight shift in the high and low stress regions. This occurred due to separate measurements being made at different times; temperatures were not consistent between the high-low stress measurements and the data for mid-range stresses.

As can be observed in the figure, only shear thinning occurs in the high stress portion of the curve. Corresponding to previous work and data obtained, the smaller particle sizes of 112 nm would show shear thickening only at much higher stresses. Moreover, higher volume fraction suspensions would probably be required to observe shear thickening. In the low stress region, the curves reach a plateau, indicating that

the suspension will still flow, even at very cold temperatures up to 4 deg. C. This result was contrary to what we had expected since colder temperatures would infinitely increase the viscosity. However, the sample at 4 deg. C was observed to be relatively "runny" and not very rigid, thus indicating that much colder temperatures are needed to observe a yield stress for the small particles.

Figures 13 through 15 are crossplots of the previous graphs mentioned. In general, the plots display anticipated trends in which higher stress viscosities are nearly stress independent due to broken particle bonds. From a comparison of these figures, curves begin to show a significant deviation at higher stresses for smaller particles. Deviations for 700 nm particles begin at approximately a stress of 2-4 Pa, whereas deviations for 112 nm particles begin at a higher stress of 8 Pa. It may be noted that low stress curves in Figure 15 show an irregularity; viscosities slightly decrease rather than increase exponentially as would have been expected.

3.5 Conclusions

Concentrated suspensions of hard sphere silica were studied to determine shear stress-dependent viscosities and its relationship to temperature variation. Volume fraction and particle size effects were observed from investigations on both 700 nm and 112 nm particle diameters samples. Overall, the data obtained followed expected trends according to theory. Very cold temperatures which induced a phase transition in the sample to very rigid suspensions effectively increased the viscosity to infinity. In addition, a higher temperature resulted in a lower viscosity at a given shear stress. Curves corresponding to various temperatures showed both shear thinning and shear thickening, depending on particle size, volume fraction, and temperature. With crossplots, high shear stress effects which break particle bonds are readily seen; viscosities become stress and temperature independent and those effects are emphasized as seen by the superimposed curves at higher temperatures.

3.6 Recommendations

In order to further characterize the effect of temperature on stress-dependent viscosities, shear stress extremes need to be investigated for the various volume

fractions at the particle diameter of 700 nm. Thus, a comparison can be made between the 112 nm and 700 nm particles. Full stress sweeps for the 112 nm particles should be reproduced for constant temperatures, thereby allowing a comparison of zero shear rate viscosity data to those obtained by Marshall and Zukoski [13]. Further analysis of data is recommended in order to investigate viscosity differences in the solvent at high stresses. Another interesting analysis would involve replotting the data on a dimensionless shear stress axis to see whether curves would superimpose. In the long run, mixtures of different particle sizes can be studied to investigate effects of temperature and shear stress on viscosities for polydisperse suspensions.

References:

[1] The Rank Pulse Shearometer, "The Simple Solution to Shear Modulus Measurements," Pen Kam, 1.0-1.10, 1986.

[2] Tadros, Tharwat F., "Rheology of Concentrated Suspensions," Chemistry and Industry, No.7, 1 April 1985, 210.

[3] Buscall, Richard, Goodwin, James W., Hawkins, Michael W., and Ottewill, Ronald H., J. Chem Soc., Faraday Trans. I, 78, 2873m 1982.

[4] Chang, Jeanne Christine, Elasticity Measurements of SiO2 Suspensions with a Bimodal Size Distribution, M.S. Thesis, University of Illinois at Urbana-Champaign, 1988.

[5] Stober, Fink, and Bohn, J. Colloid Interface Sci., 26, 62, 1968.

[6] Bogush, G.H., Tracy, M.A., Zukoski, C.F. IV., "Preparation of Monodisperse Silica Particles: Control of Size and Mass Fraction," J. Non-Crystalline Solids, 1987.

[7] Van Helden, A.K., Jansen, J.W., Vrij, A., J. Colloid and Interface Sci., 81, No. 2, 354, 1981.

[8] Jansen, J.W., De Kruif, C.G., Vrij, A., J. Colloid and Interface Sci., 114, No. 1,2, 471.481, 1986.

[9] Chen, M., Russel, W.B., "Elasticity of Sterically Stabilized Dispersions in Poor Solvents,"

[10] Bennett and Myers, Momentum, Heat, and Mass Transfer, 3rd Edition, McGraw-Hill, Inc., 1982, p.288.

[11] Woods, M.E., Krieger, I.M., J. Colloid and Interface Science, Vol. 34, No. 1, Sept. 1970, 91.

[12] Papir, Y.S., Krieger, I.M., J. Colloid and Interface Science, Vol. 34, No. 1, Sept. 1970, 126.

[13] Marshall, L., Zukoski, C.F. IV, "Flow of Dispersions Near Close Packing," Department of Chemical Engineering, University of Illinois at Urbana-Champaign. Presented at the Materials Research Society meeting, April 1989.

APPENDIX

Table 1: Shear Moduli versus volume fraction for 350 nm hard sphere silica particles

Case	*Sam. Density	G (Pa) uncorrected	G(Pa) corrected	volume fraction%
20EA	1.402	623	873.4	58.02
20EB	1.399	614	859.0	57.69
20EC	1.402	580	813.2	58.08
20ED	1.395	605	844.0	57.22
20EE	1.388	477	662.1	56.50
20EF	1.381	557	769.2	55.72
20EG	1.365	336	458.6	53.92
20EH	1.366	251	342.9	54.04
20EI	1.362	266	362.3	53.54
20EJ	1.354	272	368.3	52.59
20EK	1.351	245	331.0	52.27

*Note: Sample density was calculated from the following formula:

$$p(\text{sample}) = p(\text{silica})\S + p(\text{decalin})*(1-\S)$$

where p is density and § is volume fraction.

Table 2: Storage and Loss Components of the Shear Modulus

Case	Alpha	R	G' storage	G'' loss
20EA	.4422	.3110	4.678E+2	3.221E+2
20EB	.5771	.2304	5.242E+2	2.551E+2
20EC	.6614	.2659	4.701E+2	2.690E+2
20EE	.8134	.2894	3.721E+2	2.350E+2
20EG	.8489	.2725	269.52	158.70
20EH	1.060	.2925	194.78	124.60
20EI	1.325	.2707	213.99	125.02
20EL	1.814	.2892	146.70	92.61

Table 3: Data for temperature variation on shear moduli

Volume Fraction	Particle Size (nm)	Temperature (deg. C)	Shear Modulus(Pa)
0.464	350	-10 ± 1	∞
0.464	350	-5 ± 1	5,877
0.478	350	-1 ± 1	1,060
0.484	350	-9 ± 1	15,254
0.484	350	-8 ± 1	3,869
0.484	350	-3 ± 1	67,318
0.508	350	5 ± 1	975
0.505	700	-13 ± 1	22,176

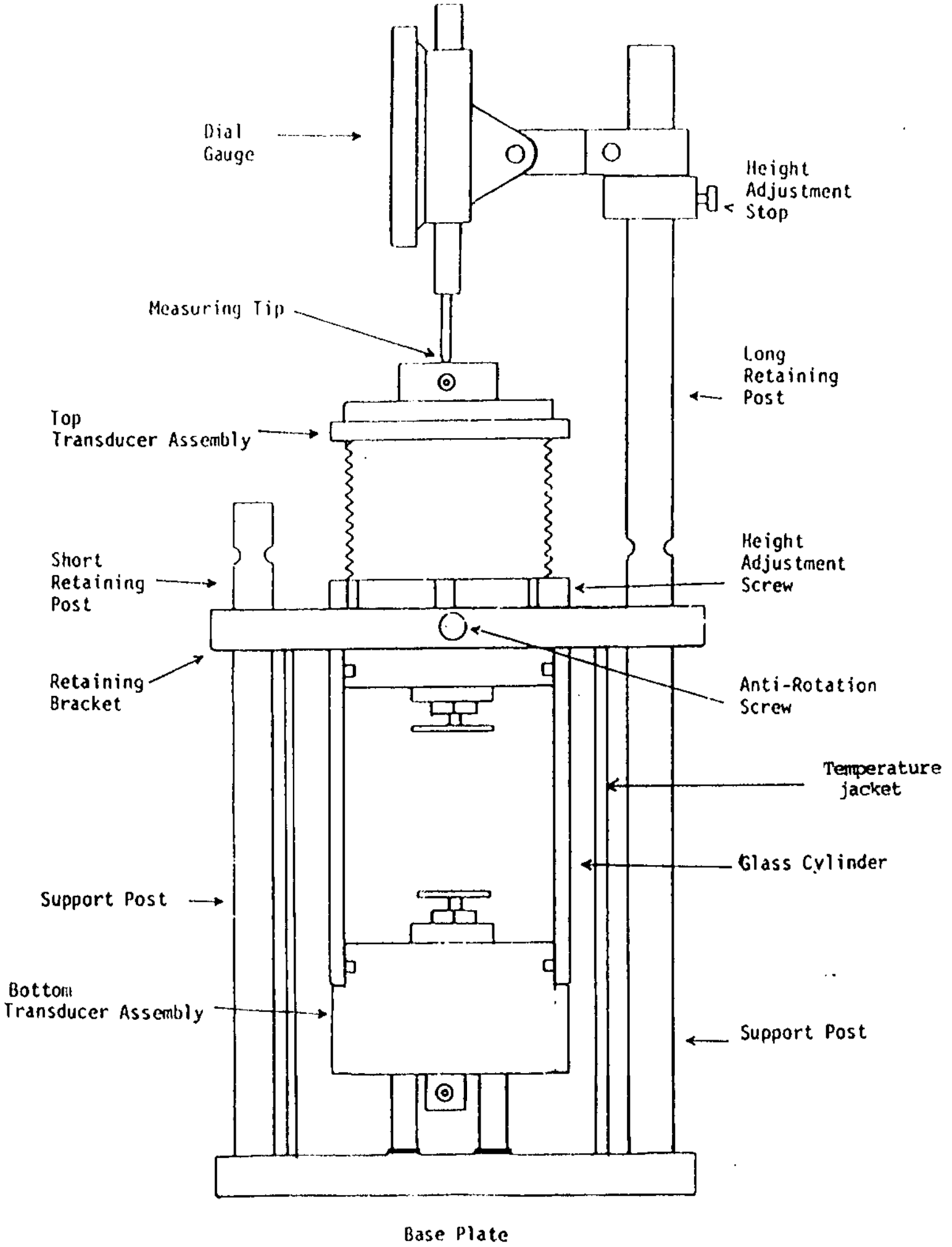

Figure 1: Apparatus of Rank Shearometer

Figure 2: Velocity curve produced by Rank Shearometer

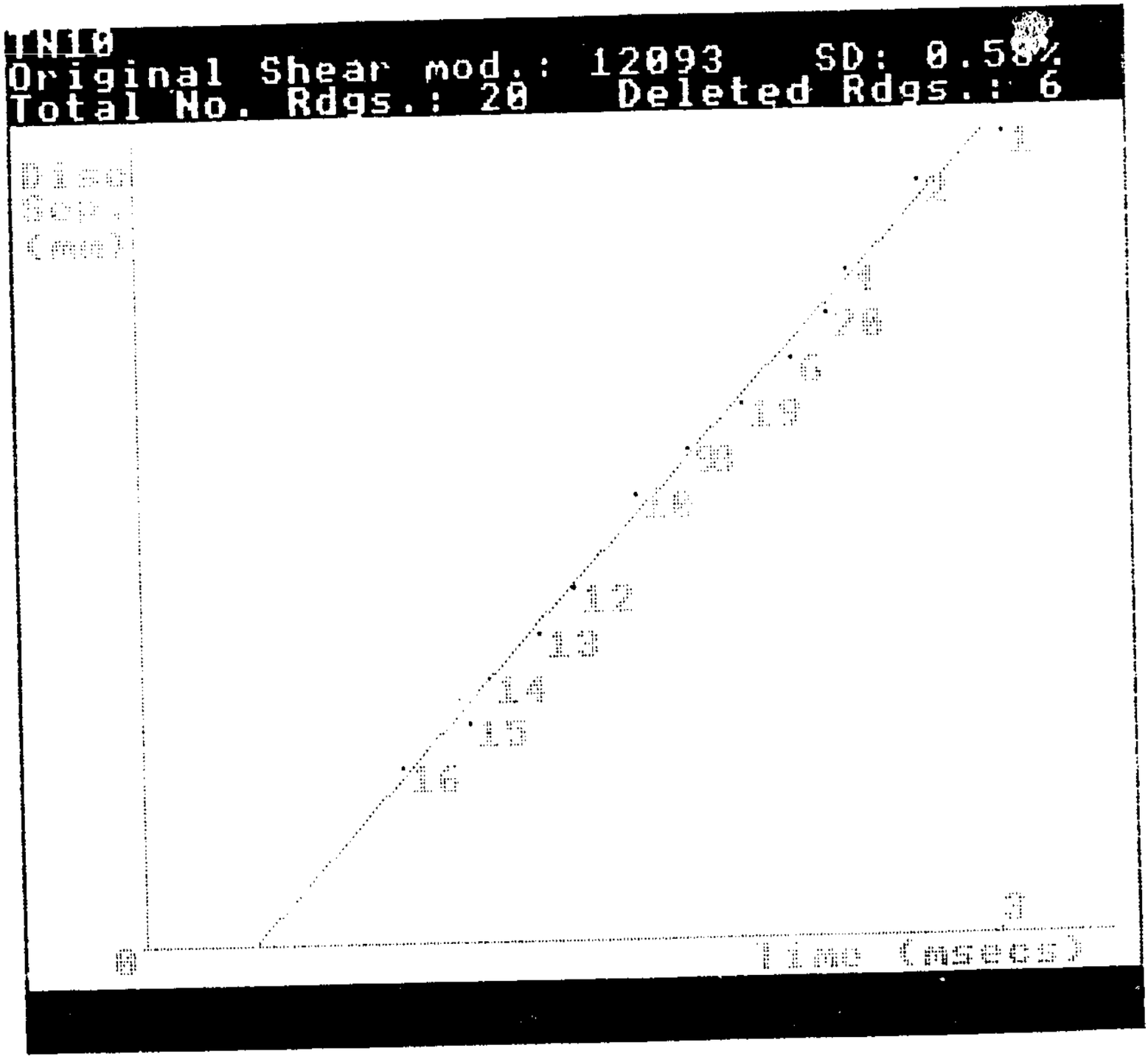

Figure 3: Shear Moduli versus Volume Fraction for 350 nm hard sphere silica particles

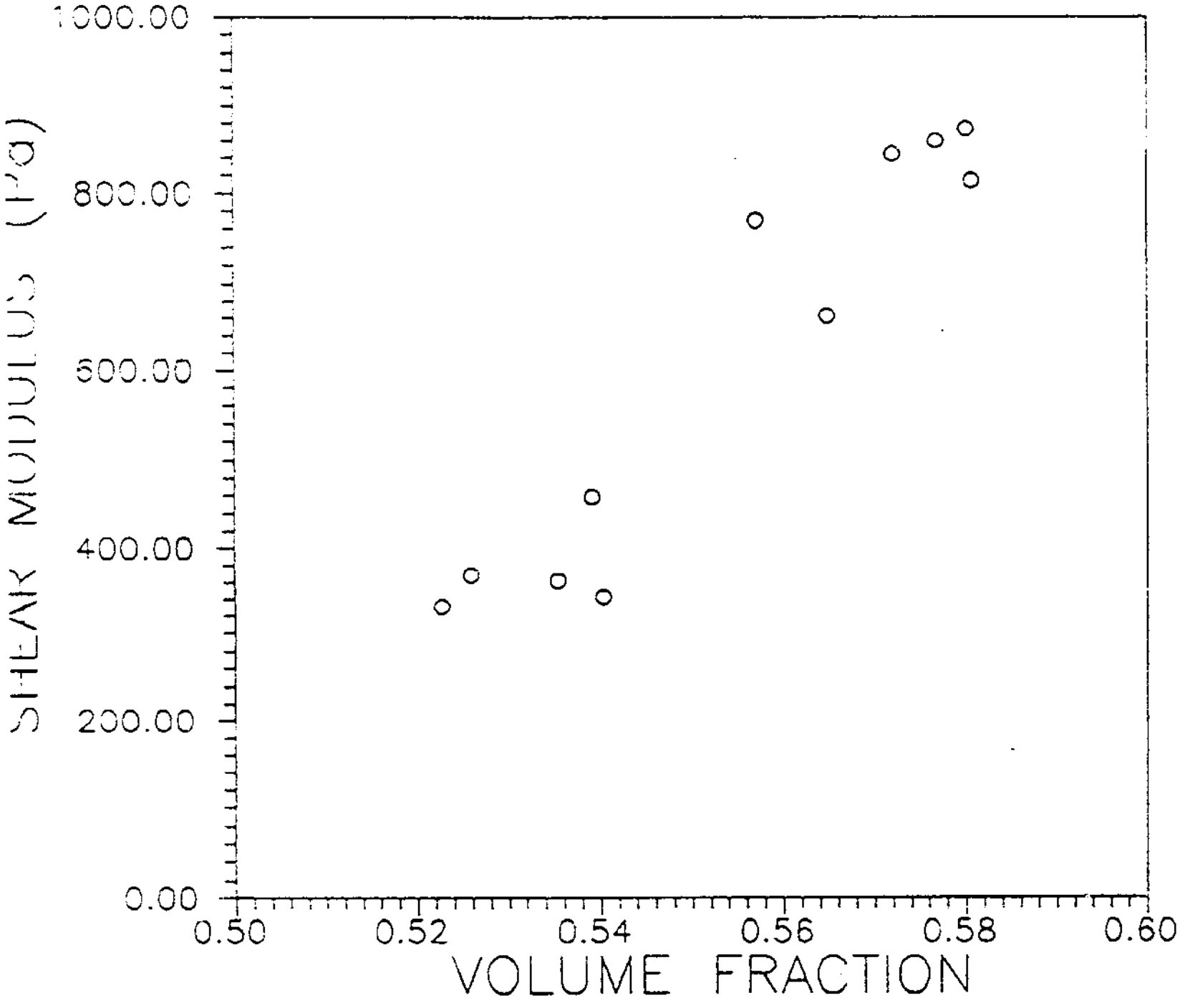

Figure 4: Shear Modulus Storage and Loss Components versus Volume Fraction for 350 nm particles

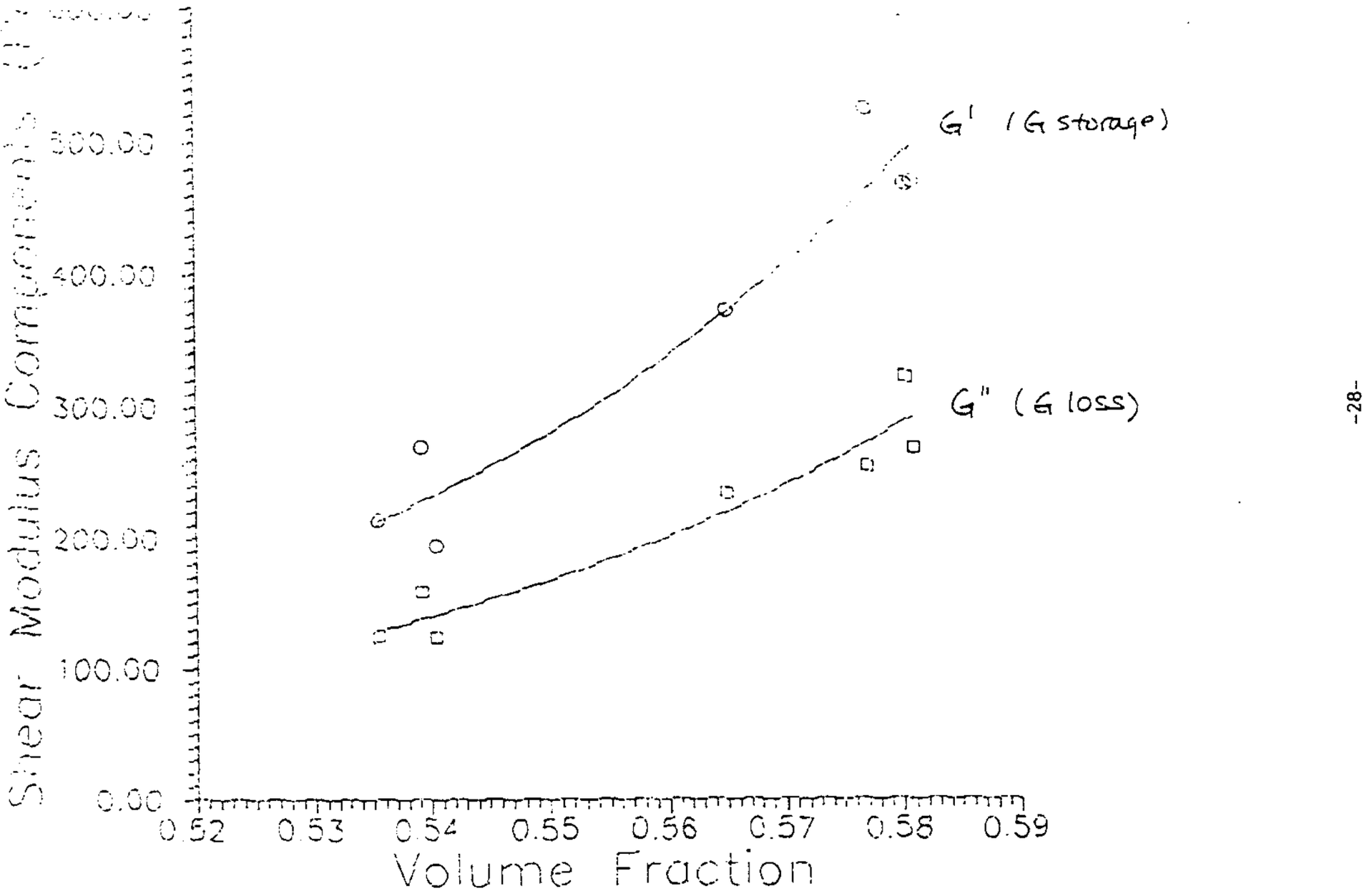

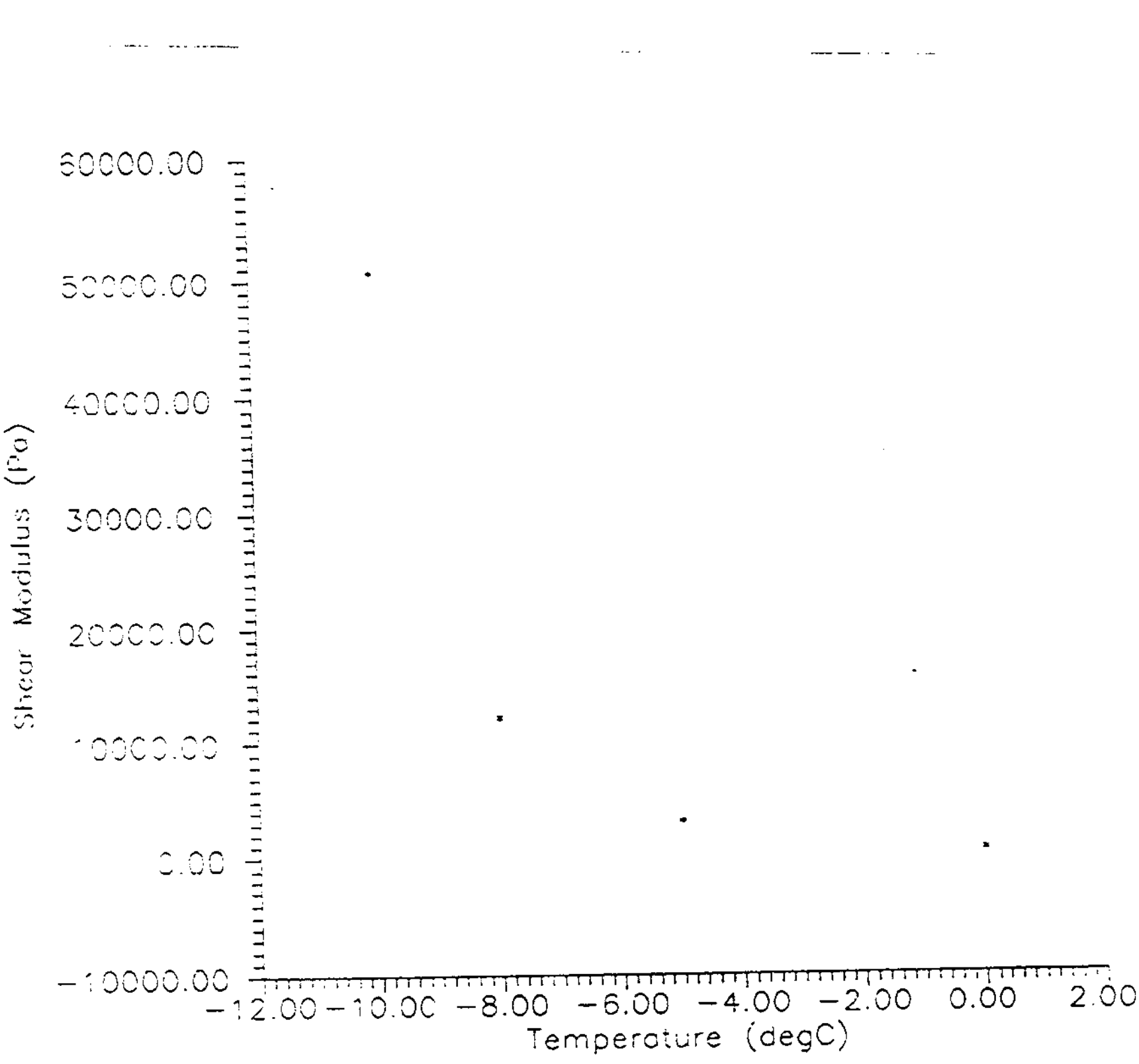

Figure 5: Shear Modulus versus Temperature for dilute sample of 350 nm hard sphere silica particles

Figure 6: Typical Viscosity versus Shear Stress Curve

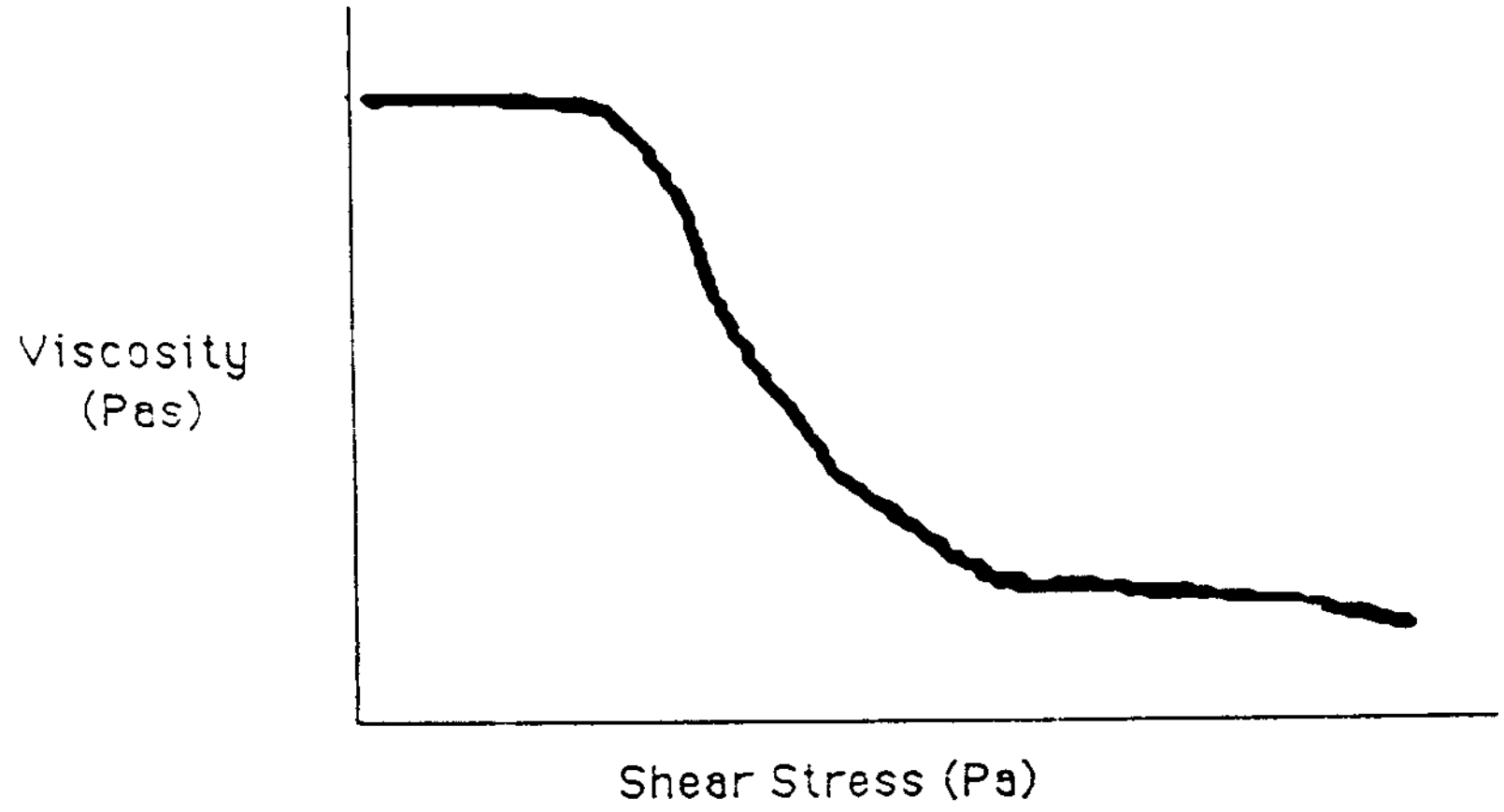

Figure 7: Viscosity versus Shear stress curve showing infinite viscosity

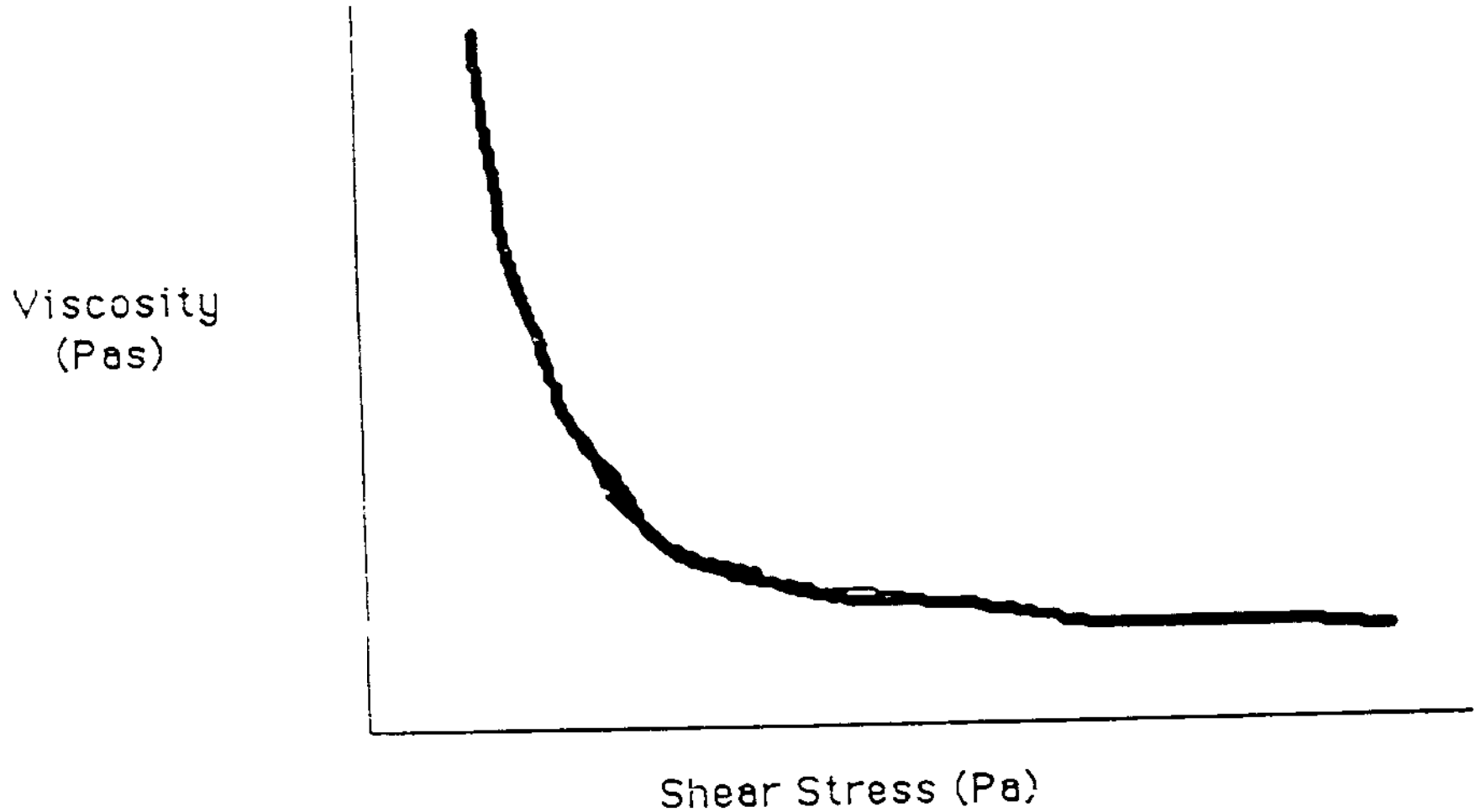

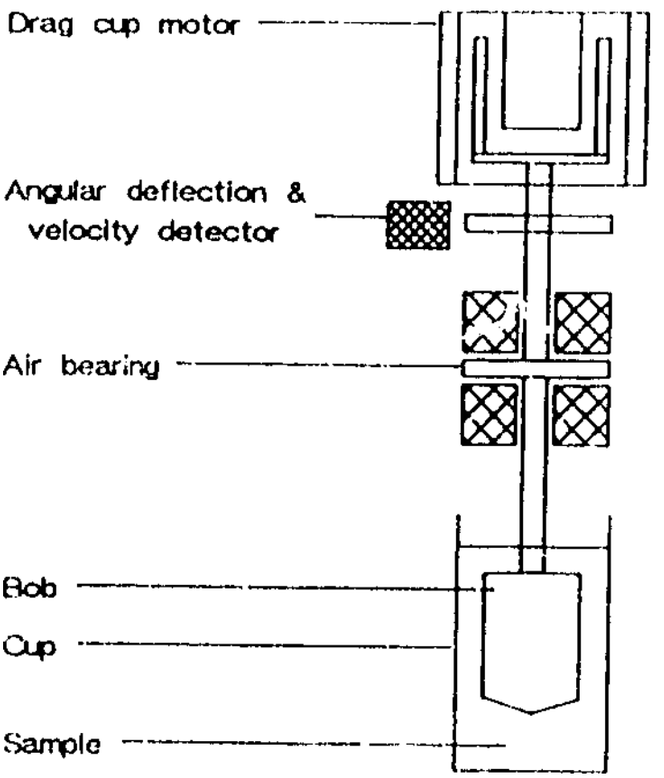

Figure 8: Apparatus of the Bohlin CS Rheometer

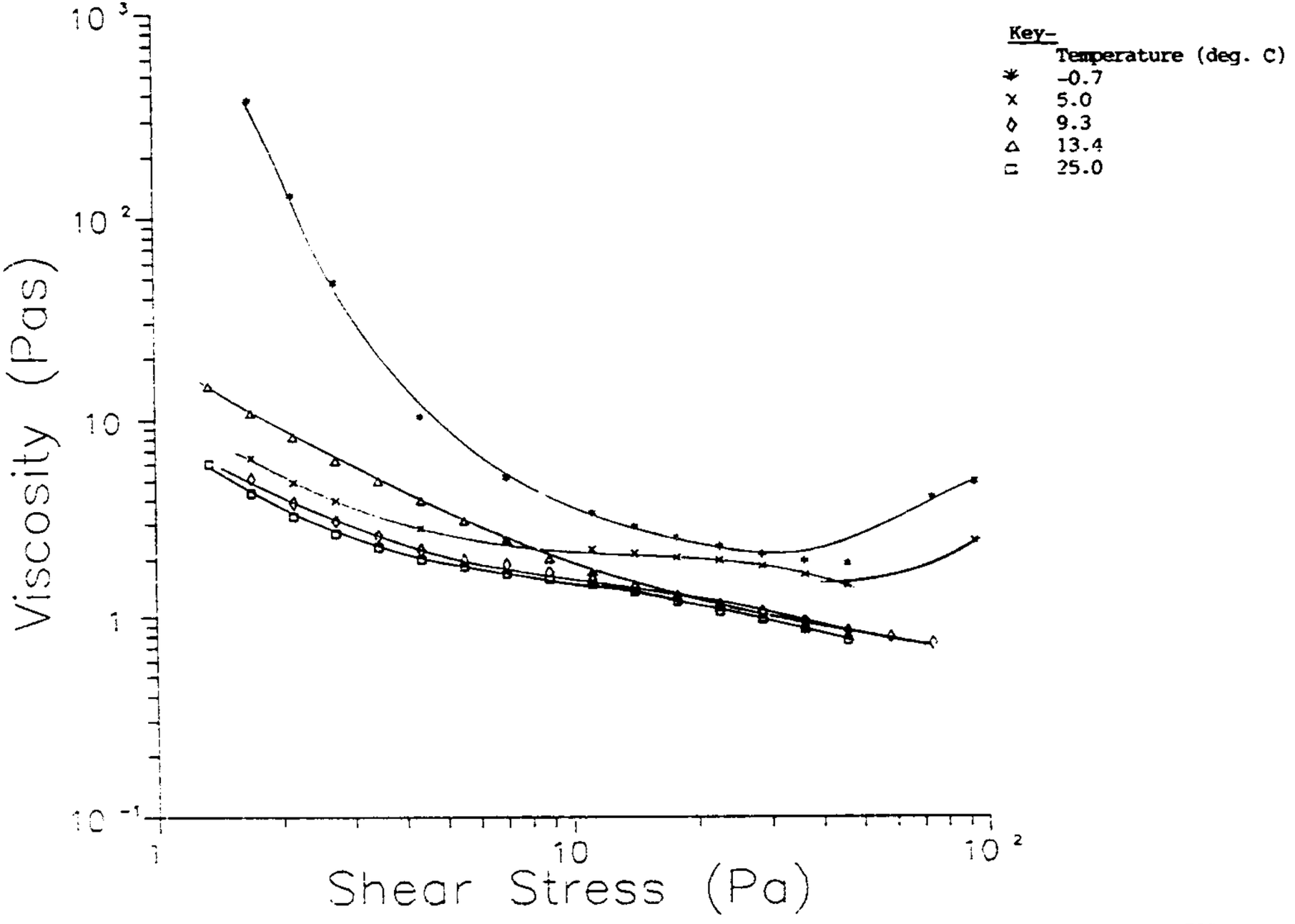

Figure 9: Viscosity versus Shear Stress curve for 0.50 volume fraction for particle diameter of 700 nm

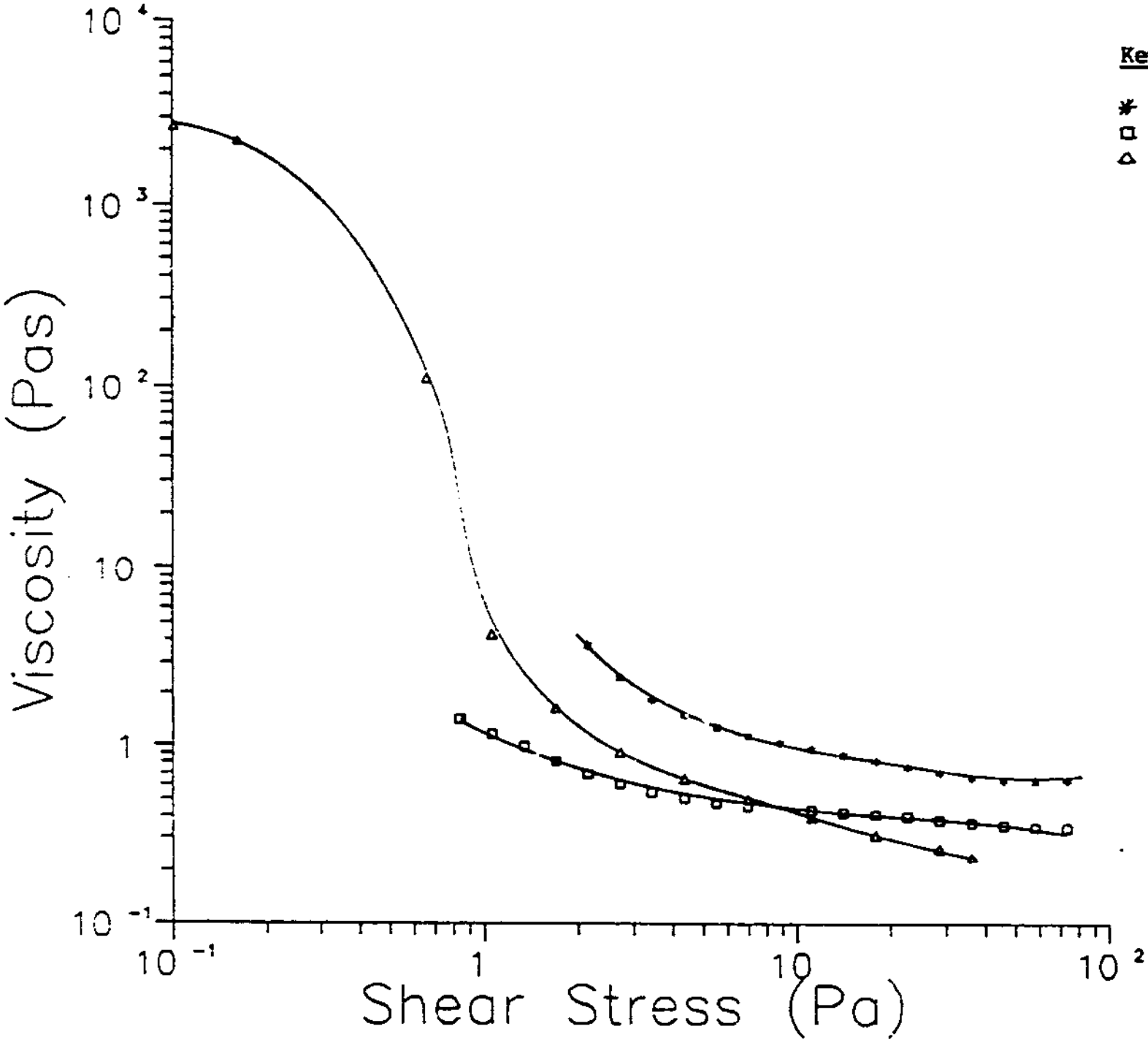

Figure 10: Viscosity versus Shear Stress curve for 0.512 volume fraction for particle diameter of 700 nm

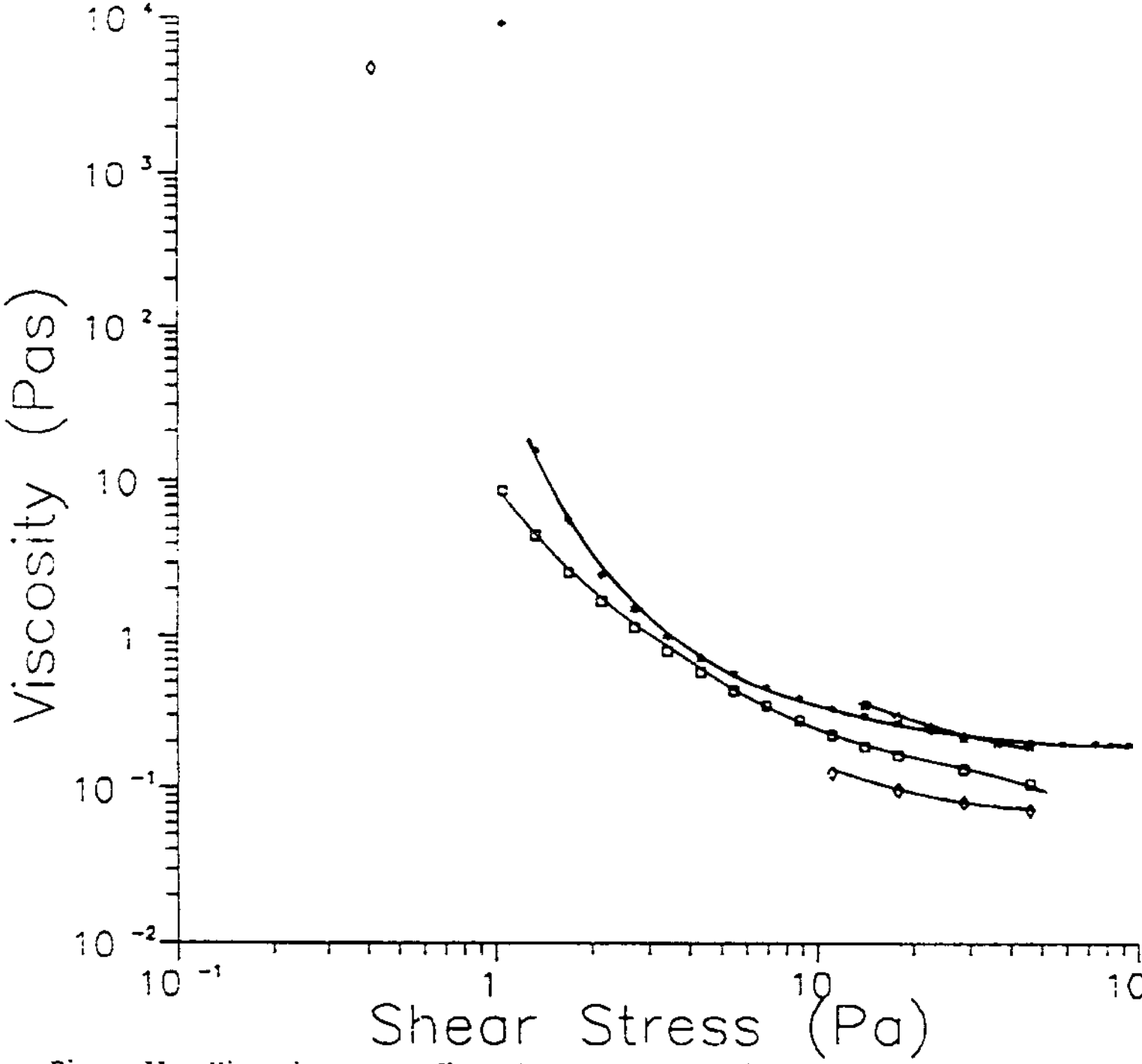

Figure 11: Viscosity versus Shear Stress curve for 0.449 volume fraction for a particle diameter of 700 nm

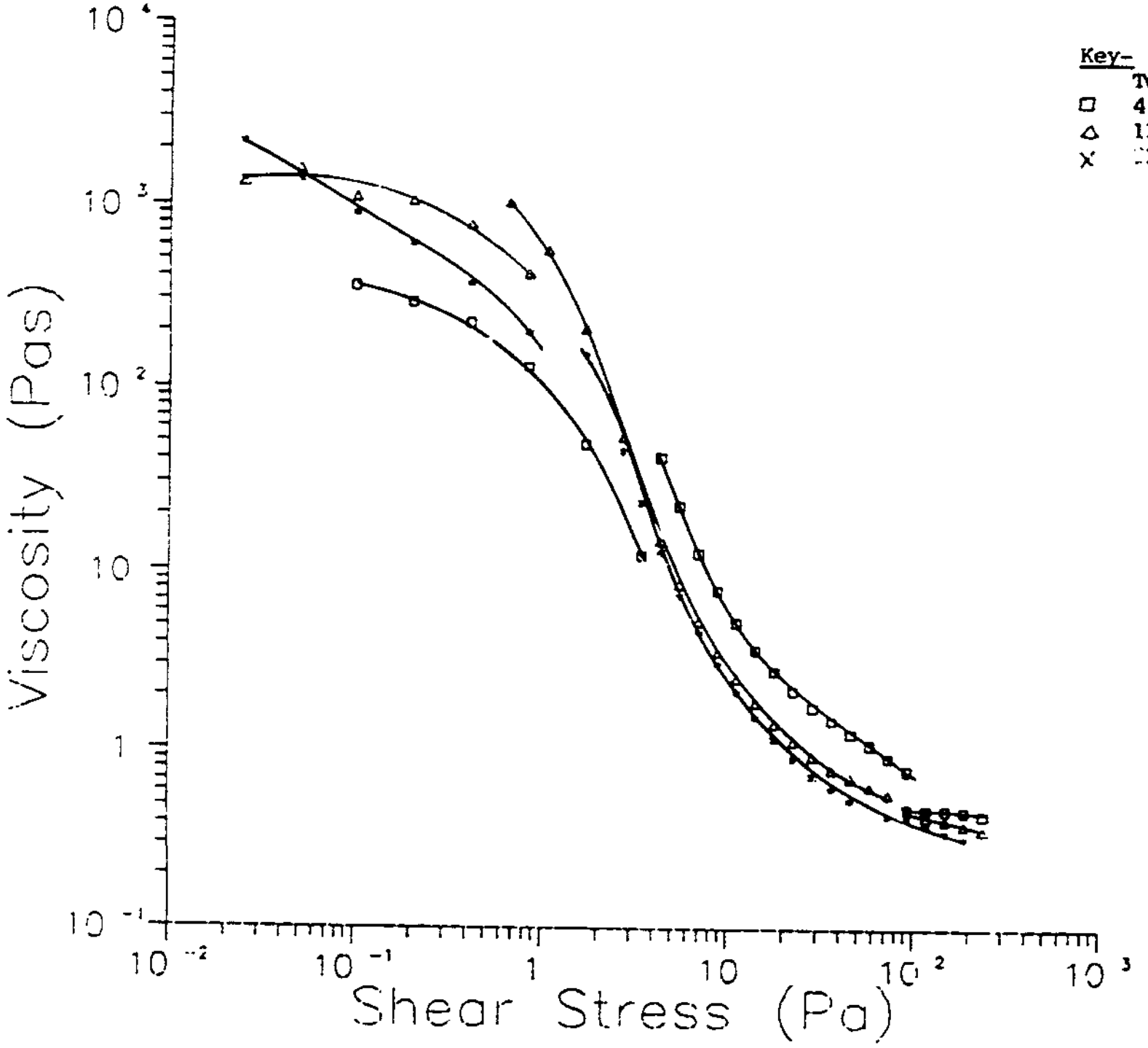

Figure 12: Viscosity versus Temperature curve at 0.489 volume fraction for a particle diameter of 112 nm

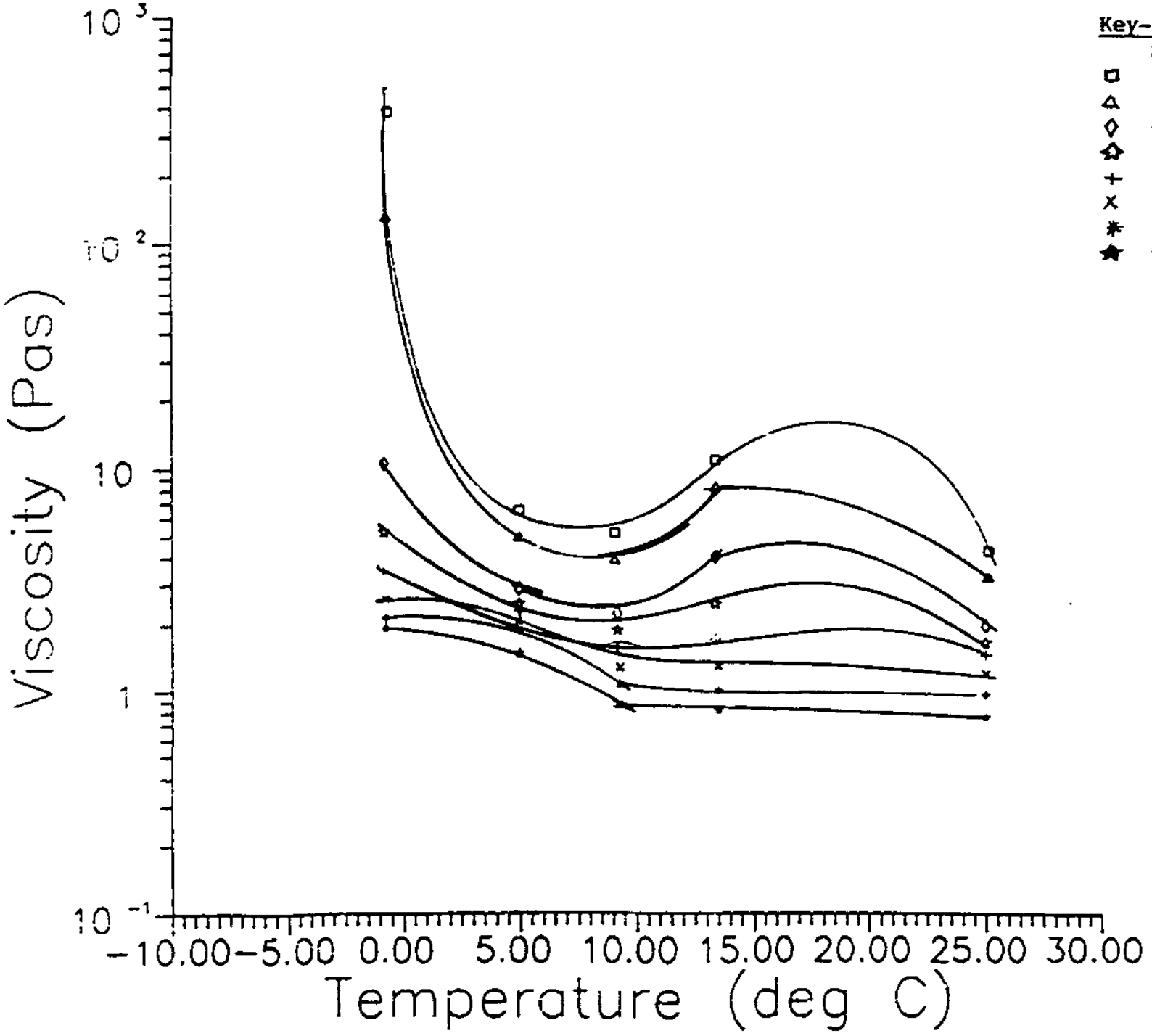

Figure 13: Viscosity versus Temperature curve at 0.50 volume fraction for a particle diameter of 700 nm

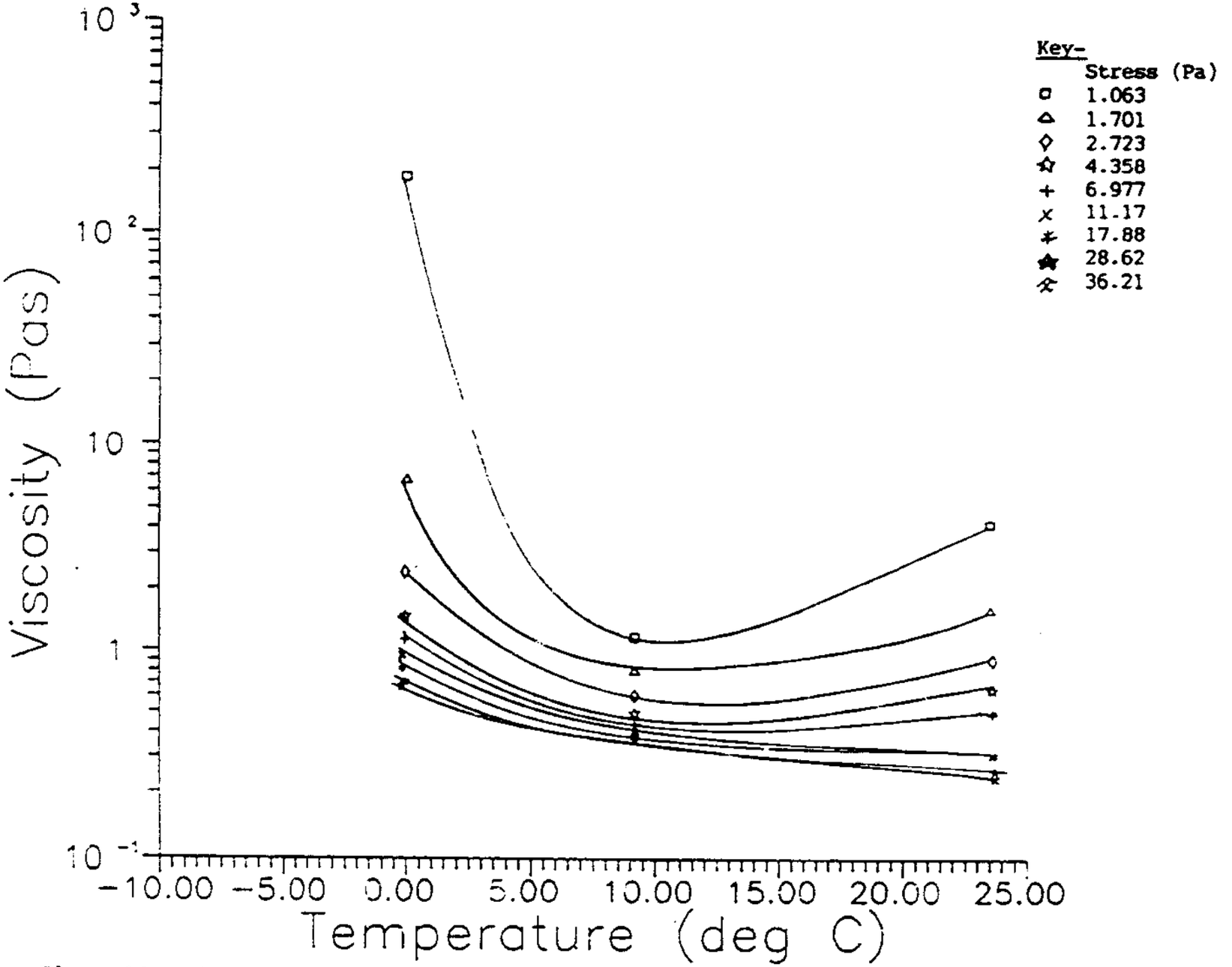

Figure 14: Viscosity versus Temperature curve at 0.512 volume fraction for a particle diameter of 700 nm

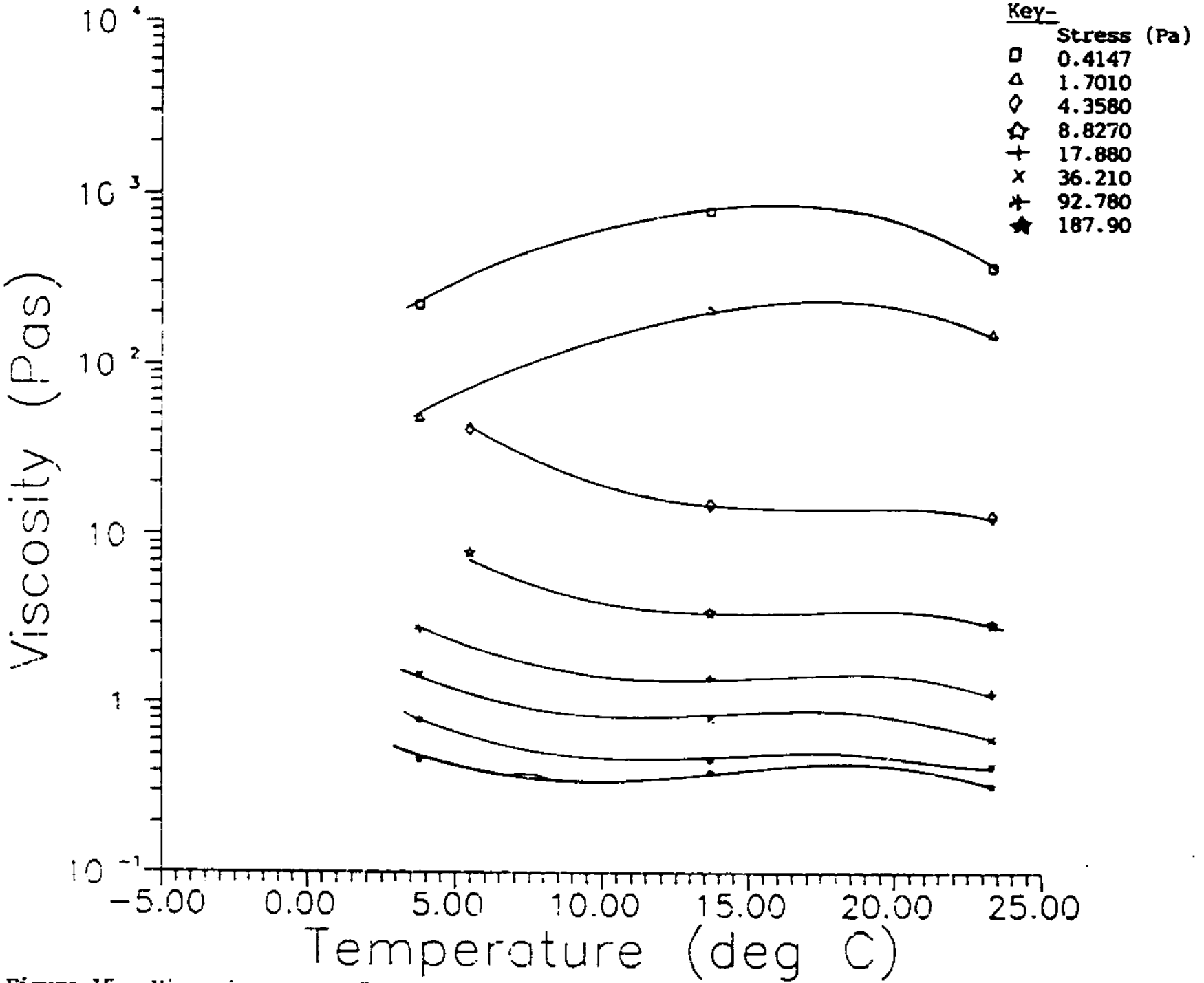

Figure 15: Viscosity versus Temperature curve at 0.489 volume fraction for a particle diameter of 112 nm